

# Effect of suction on flow of dusty fluid along exponentially stretching cylinder

Waheed Iqbal<sup>1</sup>, Mudassar Jalil<sup>2</sup>, Amjad Qazaq<sup>3</sup>, Mohamed A. Khadimallah<sup>3,4</sup>, Muhammad N. Naeem<sup>1</sup>  
Muzamal Hussain\*<sup>1</sup>, S.R. Mahmoud<sup>5</sup>, E. Ghandourah<sup>6</sup> and Abdelouahed Tounsi<sup>7,8</sup>

<sup>1</sup>Department of Mathematics, Govt. College University Faisalabad, 38000, Faisalabad, Pakistan

<sup>2</sup>Department of Mathematics, COMSATS Institute of Information Technology, Park Road, Chak Shahzad, 44000 Islamabad, Pakistan

<sup>3</sup>Prince Sattam Bin Abdulaziz University, College of Engineering, Civil Engineering Department, Al-Kharj, 16273, Saudi Arabia

<sup>4</sup>Laboratory of Systems and Applied Mechanics, Polytechnic School of Tunisia, University of Carthage, Tunis, Tunisia

<sup>5</sup>GRC Department, Faculty of Applied Studies, King Abdulaziz University, Jeddah, Saudi Arabia

<sup>6</sup>Department of Nuclear Engineering, Faculty of Engineering, King Abdulaziz University, Jeddah, Saudi Arabia

<sup>7</sup>YFL (Yonsei Frontier Lab), Yonsei University, Seoul, Korea

<sup>8</sup>Department of Civil and Environmental Engineering, King Fahd University of Petroleum & Minerals,  
31261 Dhahran, Eastern Province, Saudi Arabia

(Received September 12, 2020, Revised November 18, 2020, Accepted November 19, 2020)

**Abstract.** The present manuscript focuses the effects of suction on the flow of the dusty fluid along permeable exponentially stretching cylinder. Derived PDEs for this work are changed into ODEs by adopting right transformations. Numerical procedure is carried out for the obtained resultant equations by Shooting Technique in accordance with Runge-Kutta (RK-6) technique. Obtained results for the parameters namely, particle interaction parameter, suction parameter and Reynold number parameters are probed thoroughly. Some salient points are: (a) Fluid velocity decreases and the dust phase velocity rises for the higher values of particle interaction parameter; (b) more suction produces retarding velocities for both the phases; (c) high Reynold number slows down the fluid velocity while the speed of dust phase and (d) skin friction coefficient goes high for all these parameters.

**Keywords:** dusty fluid; stretching cylinder; similarity transformations; exponential stretching; numerical solution

## 1. Introduction

Current investigations in fluid mechanics surrounds around the variety of flow problems for different fluids along the stretching cylinder. The main cause behind the immense interest of researchers is vast implementation of this phenomenon in lot of industrial and engineering processes for the sake of advancement in the techniques like manufacturing of metallic and plastic fiber sheets, making of copper wires, fabrication of electronic components, designing of water supply network and many more.

Firstly, Wang (1988) studied the fluid behavior along the stretching cylinder. The detailed study of fluid flow along the stretched cylinder for the boundary layer was made Ishak and Nazar (2009) regarding. Wang and Ng (2011) obtained the asymptotic solutions for high Reynold number using slip flow condition. Mixed convection condition together with slip flow and obtained numerical solution for the boundary layer problem of Williamson fluid flow over a stretching cylinder (Salahuddin *et al.* 2017). The effects of Soret and Dufour for the Casson fluid by considering the heat transfer along stretching cylinder was worked out (Mahdy 2015). The mass and convective heat conditions for

Casson fluid flow having nanoparticles along stretching cylinder was presented (Imtiaz *et al.* 2016). A thorough numerical study of sisko fluid flow over stretching cylinder with effects of thermal conductivity and viscous dissipation was done (Malik *et al.* 2016). Al-Maliki *et al.* (2020) carried out the dynamic analysis of Functionally Graded (FG) graphene-reinforced beams under thermal loading based on finite element approach. The presented formulation is based on a higher order refined beam element accounting for shear deformations. The graphene-reinforced beam is exposed to transverse periodic mechanical loading.

The uniform suction/blowing effects together with transfer of heat outside the permeable stretching cylinder were considered (Ishak *et al.* 2008). Under convective boundary conditions, electrically conducting sisko fluid along the stretching cylinder in axial direction was probed (Khan and Malik 2015). They found the considerable boost in the flow parameters for shear thinning than thickening. The notable point about all the above mentioned studies is that the considered fluid is "Pure". Practically it is almost impossible to have such fluid which is free from any kind of impurity. Every naturally occurring fluid contains dust particles. Many engineering and industrial problems deal with dusty fluid such as powder mechanization and centrifugal technique to the detachment of particles from the fluid. Flow of dusty fluid can be viewed in many natural phenomena e.g., flow of mud in rivers, blood flow and atmospheric flow during haze. Initiative study of motion of

\*Corresponding author, Ph.D. Scholar,  
E-mail: muzamal45@gmail.com;  
muzamalhussain@gcuf.edu.pk

dust particles in laminar flow has been carried out (Saffman 1962). An analysis for viscous, incompressible steady flow of dusty fluid flowing between two co-axial rotating cylinders under pressure gradient effect was carried out (Nath 1970). Akgoz and Civalek (2011) investigated geometrically the nonlinear free vibration analysis of thin laminated plates resting on non-linear elastic foundations. Winkler-Pasternak type foundation model is used. Governing equations of motions are obtained using the von Karman type nonlinear theory. The method of discrete singular convolution is used to obtain the discretised equations of motion of plates. Akbaş (2015) conducted the effect of material-temperature dependent on the wave propagation of a cantilever beam composed of Functionally Graded Material (FGM) under the effect of an impact force. The beam is excited by a transverse triangular force impulse modulated by a harmonic motion. Material properties of the beam are temperature-dependent and change in the thickness direction. Sharma *et al.* (2018e) presented the novel higher-order coupled finite-boundary element scheme for the computation of the thermoacoustic responses of the layered panel structure under the harmonic excitation. The thermally pre-stressed vibrating composite panel model is derived mathematically using the higher-order shear deformation mid-plane kinematics. Akbaş (2017a) investigated the free vibration analysis of edge cracked cantilever microscale beams composed of FGM used on the Modified Couple Stress Theory (MCST). The material properties of the beam are assumed to change in the height direction according to the exponential distribution. Batou *et al.* (2019) studied the wave propagations in Sigmoid Functionally Graded (S-FG) plates using new Higher Shear Deformation Theory (HSDT) based on two-dimensional (2D) elasticity theory. The current higher order theory has only four unknowns, which mean that few numbers of unknowns, compared with first shear deformations and others higher shear deformations theories and without needing shear corrector.

Baaskaran *et al.* (2018) studied the reliable and accurate method of computationally aided design processes of advanced thin walled structures in automotive industries for the efficient usage of smart materials, that possess higher energy absorption in dynamic compression loading. The most versatile components i.e., thin walled crash tubes with different geometrical profiles are introduced in view of mitigating the impact of varying cross section in crash behavior and energy absorption characteristics. Akbaş (2018a, b, c) analyzed the objective of large deflections of a fiber reinforced composite cantilever beam under point loads. In the solution of the problem, finite element method is used in conjunction with 2D continuum model. It is known that large deflection problems are geometrically nonlinear problems. In the nonlinear model of the laminated beam, total Lagrangian finite element model of is used in conjunction with the Timoshenko beam theory.

Sharma *et al.* (2018c, d) carried out numerically the acoustic radiation responses of doubly curved laminated composite shell panels subjected to harmonic excitation are investigated numerically in the framework of the higher-order shear deformation theory. A general mathematical

model for the vibrating curved panel has been developed and the cylindrical, spherical, elliptical and hyperboloid shell panel geometries resting on an infinite rigid baffle are considered for analysis. A numerical scheme for the vibrating plate has been developed in the framework of the higher-order mid-plane kinematics and the eigen frequencies are obtained by employing suitable finite element steps. Dusty gas flow in a region occupied by boundary layer was examined (Chakrabarti 1974). Akbaş (2019a, b, c) investigated the geometrically nonlinear static analysis and post buckling of laminated composite beams under hygrothermal effect. The finite element method is used within the first shear beam theory. Total Lagrangian approach is used nonlinear kinematic model. The geometrically nonlinear formulations are developed for the laminated beams with hygro-thermal effects. The coefficient of friction and heat transfer for dusty boundary layer flow with pressure gradient was studied (Agranat 1988). In addition to these studies for flow and transfer of heat for dusty fluid along sheet/surface, many researchers considered dusty fluid flow along cylinder. The viscous, incompressible gas flow having dust particles for an isothermal cylinder was discussed and results from various physical parameters were presented (Rebhi 2010). Yüksel and Akbaş (2019) studied the fiber-reinforced laminated composites that are frequently preferred in many engineering projects. With the development in production technology, the using of the fiber reinforced laminated composites has been increasing in engineering applications. In the production stage of the fiber-reinforced laminated composites, porosities could be occurred due to production or technical errors. Chen *et al.* (2019a, b) carried the energy absorption characteristics of a Lattice-web Reinforced Composite Sandwich Cylinder (LRCSC) which is composed of Glass Fiber Reinforced Polymer (GFRP) face sheets, GFRP lattice webs, polyurethane (PU) foam and ceramsite filler. The vortex-induced vibration of three circular cylinders (each of diameter  $D$ ) in an equilateral triangular arrangement is investigated using the immersed boundary method.

Abdulrazzaq *et al.* (2020) investigated the thermo-elastic buckling of small scale FGM nano-size plates with clamped edge conditions rested on an elastic substrate exposed to uniformly, linearly and non-linearly temperature distributions employing a secant function based refined theory. Material properties of the FGM nano-size plate have exponential gradation across the plate thickness. Civalek (2017) investigated the free vibration analysis of conical and cylindrical shells and annular plates made of composite laminated and FGMs. The Carbon Nanotubes Reinforced (CNTR) composite case is also taken consideration for FGM. The equations of motion for conical shell are obtained via Hamilton's principle using the transverse shear deformation theory. Akbaş (2020a) studied the dynamic responses of laminated composite beams under a moving load with thermal effects. The governing equations of problem are derived by using the Lagrange procedure. The transverse-shear strain and rotary inertia are considered within the Timoshenko beam theory. The material properties of laminas are considered as the

temperature dependent physical property.

Sharma *et al.* (2018a, b) studied the vibroacoustic responses of laminated composite curved panels subjected to harmonic point excitation in a combined temperature and moisture environment using a novel higher-order finite-boundary element model. The hygro-thermal dependent composite material properties are incorporated macroscopically in the formulation. The natural frequencies alongside corresponding modes of the flat panels resting on an infinite rigid baffle are obtained by using finite element method in the framework of the higher-order shear deformation theory. Some valuable results regarding heat transfer of dusty fluid over a hollow stretching cylinder using multi-step DTM were reported (Rasekh *et al.* 2014). Conduction of dusty fluid flow along stretching cylinder with thermal conductivity and viscosity effects were dealt numerically (Konch and Hazarika 2017).

Derakhshandeh *et al.* (2020) investigated the Reynolds number  $Re (= 50-200)$  effects on the flows around a single cylinder and the two tandem (center-to-center spacing  $L^* = L/D = 4$ ) cylinders, each of a diameter  $D$ . Vorticity structures, Strouhal numbers, and time-mean and fluctuating forces are presented and discussed. Sharma *et al.* (2017a, b, c) investigated the vibro-acoustic responses of the laminated composite flat panel in an infinite rigid baffle under the influence of central and eccentric harmonic point excitation. A general mathematical model of the flat panel is developed in the framework of the higher order shear deformation theory to compute the vibrational properties. The frequency values of the panel are obtained by using simulation model through the commercial finite element package (ANSYS) via batch input technique. The structural responses are obtained using a simulation model via ANSYS including the effect various geometries (cylindrical, elliptical, spherical and hyperboloid). Initially, the model has been established by solving adequate number of available examples to show the convergence and comparison behaviour of the natural frequencies. Akbaş (2020b) studied the axially damped forced vibration responses of viscoelastic nanorods within the frame of the modal analysis. The nonlocal elasticity theory is used in the constitutive relation of the nanorod with the Kelvin-Voigt viscoelastic model. In the forced vibration problem, a cantilever nanorod subjected to a harmonic load at the free end of the nanorod is considered in the numerical examples. Salah *et al.* (2019) employed a simple four-variable integral plate theory for examining the thermal buckling properties of FGM sandwich plates. The proposed kinematics considers integral terms which include the effect of transverse shear deformations. In some fresh attempts, the researchers have pondered over new dimensions of stretching i.e., exponentially stretching cylinder. The detailed study of flow and transfer of heat for hyperbolic tangent fluid over a stretching cylinder exponentially in vertical direction was carried out (Naseer *et al.* 2014). Shadravan *et al.* (2019) performed lateral load testing on seventeen wood wall frames in two sections. Section one included eight tests studying structural foam sheathing of shear walls subjected to monotonic loads following the ASTM E564 test method.

Similarity solution has been derived for steady boundary layer and heat flow of Casson nanofluid (Malik *et al.* 2013) while cylinder was stretching exponentially along its radius. The flow of Micropolar fluid through vertical exponentially stretching cylinder along the axial direction and discussed heat transfer effects, too, were considered (Rehman 2015). Williamson fluid flow along an exponentially stretching cylinder was examined and they found its numerical solution (Iqbal *et al.* 2019). Recently some researcher used different methods for nonlinear modeling (Avcar 2019, Karami *et al.* 2017, 2018, Madani *et al.* 2016, Simsek 2011) and some other methods as open see softare (Moghaddam and Masoodi 2019), first order shear deformation theory (Loghman *et al.* 2018), MLPG method (Rad *et al.* 2020), Ritz-type variational method (Sofiyev *et al.* 2006), multiphysical numerical (FE-BE) solution and higher-order shear theory (Sharma and Panda 2020, Sharma *et al.* 2019a, b, 2020) and for nonlinear modeling (Eltaher *et al.* 2019, Ebrahimi *et al.* 2019, Safaei *et al.* 2019, Shahsavari *et al.* 2019, Benmansour *et al.* 2019); Newton-Raphson iteration method (Akbaş 2017b, 2018c, d) and the Hamilton procedure (Akbaş 2019d).

The suggested method to investigate the flow and heat transfer effects of a dusty fluid along exponentially stretching cylinder is Runge-Kutta method, which is a well-known and efficient technique to develop the fundamental frequency equations. This method converges fast than other methods. It is keenly seen from the literature, no evidence is found concerning current model. The transformed equations are solved numerically using shooting technique with Runge-Kutta method getting inspiration from above mentioned researches, we present the work on flow of dusty fluid along an exponentially stretching permeable cylinder with suction effect. According to our information's, no such type of investigations has been done before.

## 2. Description of the problem

Consider laminar, steady, viscous, incompressible boundary layer flow of dusty fluid in two dimensions along a permeable cylinder. The cylinder is stretching exponentially along positive  $z$ -axis with velocity  $W_w = 2ace^{z/a}$ , where  $c$  is the stretching rate. The  $z$ -axis is considered along the axis of the cylinder, while  $r$ -axis is assumed perpendicular to the axial direction. Under these suppositions along the Boussinesq and the boundary layer approximation the governing equations for the flow behavior are

$$\frac{\partial(rw)}{\partial z} + \frac{\partial(ru)}{\partial r} = 0, \quad \Leftrightarrow \Leftrightarrow \quad (1)$$

$$w \frac{\partial w}{\partial z} + u \frac{\partial w}{\partial r} = \nu \left( \frac{\partial^2 w}{\partial r^2} + \frac{1}{r} \frac{\partial w}{\partial r} \right) + \frac{KN}{\rho} (w_p - w) \quad (2)$$

$$w_p \frac{\partial w_p}{\partial z} + u_p \frac{\partial w_p}{\partial r} = \frac{K}{m} (w - w_p) \quad (3)$$

$$\frac{\partial(rw_p)}{\partial z} + \frac{\partial(ru_p)}{\partial r} = 0, \quad \Leftrightarrow \Leftrightarrow \quad (4)$$

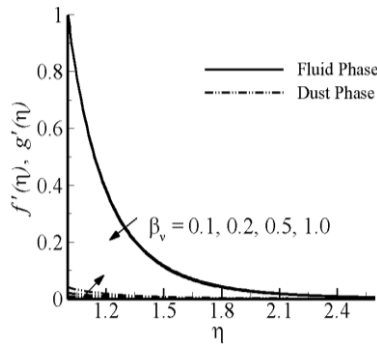


Fig. 1 Impact of particle interaction parameter on profile of velocity

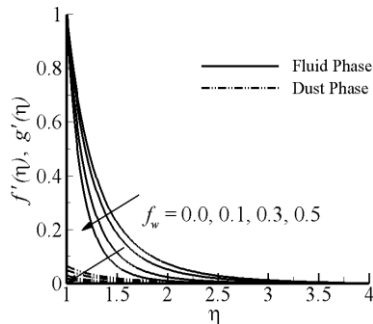


Fig. 2 Impact of suction on profile of velocity

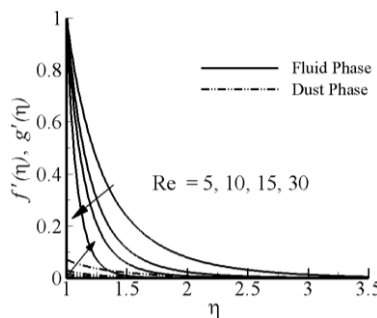


Fig. 3 Impact of Reynolds number on profile of velocity

The components of velocity of the fluid and the dust particles are  $(u, w)$  and  $(u_p, w_p)$  respectively in  $(r, z)$  directions. Parameter  $\gamma (= mN/\rho)$  denotes the mass concentration of dust particles,  $\tau = m/K$  is the relaxation time of particle phase, Here,  $\rho$  and  $\nu$  are density and kinematic viscosity of the fluid, respectively. Dusty fluid parameters  $K, N$  and  $m$  are the Stoke's resistance, number density and mass concentration of dust particle. The problem related boundary conditions are

$$\begin{aligned} r = a; & \quad w = W_w, u = U_w \\ r \rightarrow \infty; & \quad w = 0, \quad w_p = 0, \quad u_p = u \end{aligned} \quad (5)$$

here  $U_w = -a\kappa e^{z/a}$  is suction velocity with  $\kappa > 0$  corresponds to mass suction and  $\kappa < 0$  corresponds to mass injection. Eqs. (1)-(4) are non-linear coupled PDEs. These equations can easily be transformed into set of ODEs by using similarity transformations

$$\begin{aligned} \zeta = \left(\frac{r}{a}\right)^2, \quad u = -\frac{1}{2}W_w \frac{g(\zeta)}{\sqrt{\zeta}}, \quad w = W_w g'(\zeta) \\ \rho_r = R(\zeta), \quad u_p = -\frac{1}{2}W_w \frac{h(\zeta)}{\sqrt{\zeta}}, \quad w_p = W_w h'(\zeta) \end{aligned} \quad (6)$$

where the differentiation w.r.t.  $\zeta$  is denoted by prime. By using the above similarity transformation, Eqs. (1) and (5) are identically satisfied and other equations are transformed to

$$\zeta g''' + g'' + Re(gg'' - g'^2) + \beta_v \gamma (h' - g') = 0 \quad (7)$$

$$Re(hh'' - h'^2) + \beta_v (g' - h') = 0 \quad (8)$$

where the non-dimensional dusty fluid parameters  $\beta_v, \gamma$  and  $Re$  are defined as

$$\beta_v = \frac{a^2}{4\nu\tau}, \quad \gamma = \frac{mN}{\rho}, \quad Re = \frac{aU_w}{4\nu} \quad (9)$$

The above three parameters are fluid particle interaction, mass concentration and Reynold number, respectively. The relaxation time  $\tau = m/K$  of particle phase.

$$\begin{aligned} g(1) = \kappa, \quad g'(1) = 1, \quad g'(\infty) = 0 \\ h'(\zeta) = 0, \quad h(\zeta) = g(\zeta) \quad \text{as } \zeta \rightarrow \infty \end{aligned} \quad (10)$$

$C_f$  and  $\tau_w$  are skin fraction coefficient and shear stress respectively, where

$$C_f = \frac{-\tau_w}{\rho U_w^2 / 2} \quad (11)$$

$$\tau_w = \mu \left( \frac{\partial w}{\partial r} \right) \Big|_{r=a} \quad (12)$$

Using the similarity transformation Eq. (6) in Eq. (12) and substituting it in Eq. (11), the dimensionless skin friction coefficient is achieved like

$$C_f Re = -g''(1) \quad (13)$$

Eqs. (7) and (8) are non-linear coupled ordinary differential equations. Exact analytical solution of these equations is not possible; therefore, in the coming section numerical results of the problem are discussed and presented.

### 3. Results and discussions

Numerical results are shown through graphs and tables. Shooting technique by RK-Method of the sixth order is applied on derived equations. Three physical parameters i.e., particle interaction parameter ( $\beta_v$ ), suction parameter ( $f_w$ ) and the local Reynold number ( $Re$ ) are investigated on velocity profile and elaborated through proper graphs and tables. The impact of different physical parameters on velocity and temperature profile is discussed and shown graphically. Flow parameters (Figs. 1-3) like particle

Table 1 For different values of  $Re$ ,  $\beta_v$  and  $f_w$  numerical value of  $-g''(1)$ 

| $Re$ | $\beta_v$ | $f_w$ | $-g''(1)$ |
|------|-----------|-------|-----------|
| 5    | 0.7       | 0.3   | 3.408039  |
| 10   |           |       | 5.232848  |
| 15   |           |       | 6.924929  |
| 30   |           |       | 11.725938 |
| 10   | 0.1       |       | 5.144982  |
|      | 0.2       |       | 5.160159  |
|      | 0.5       |       | 5.204388  |
|      | 1         |       | 5.274110  |
|      |           | 0.0   | 3.453371  |
|      |           | 0.1   | 3.979997  |
|      |           | 0.3   | 5.232848  |
|      |           | 0.5   | 6.713866  |

Table 2 For various values of  $Re$ ,  $\beta_v$ ,  $\gamma$  and  $\delta$  numerical values of  $-\theta'(1)$ 

| $Re$ | $\beta_v$ | $\gamma$ |
|------|-----------|----------|
| 5    | 2         | 1        |
| 10   |           |          |
| 15   |           |          |
| 30   |           |          |
| 50   |           |          |
| 10   | 0.1       |          |
|      | 0.2       |          |
|      | 0.5       |          |
|      | 1         |          |
|      | 2         |          |
|      |           | 0.1      |
|      |           | 0.2      |
|      |           | 0.5      |
|      |           | 0.7      |
|      |           | 1.0      |

interaction parameter ( $\beta_v$ ), suction parameter ( $f_w$ ) and the local Reynold number ( $Re$ ) are well-portrayed on velocity profile for both the dust and the fluid phases. For calculating the numerical solution depicted by Figs. 1-3, the values of parameters are taken as  $\beta_v = 0.7$ ,  $f_w = 0.3$ ,  $\gamma = 1$  and  $Re = 10$ ,

Fig. 1 shows the behavior of increasing particle interaction parameter on velocity profile. Dust particle velocity trending high while retardation in fluid velocity is seen. Actually, the chances of interaction between dust and fluid increases for higher values of particle interaction parameter, which results in ultimate increase in dust phase velocity until the relative velocity for both the phases becomes equal. Suspension of dust particles enhances due to greater values of  $\beta_v$  and generates more internal friction. Due to this fact, fluid velocity slows down. Increasing

Table 3 For different values of  $Re$ ,  $\beta_v$  and  $\gamma$  numerical value of  $g''(1)$ 

| $Re$ | $\beta_v$ | $\gamma$ | $-g''(1)$ |
|------|-----------|----------|-----------|
| 5    | 2         | 1        | 2.741649  |
| 10   |           |          | 3.612068  |
| 15   |           |          | 4.287201  |
| 30   |           |          | 5.834313  |
| 50   |           |          | 7.392431  |
| 10   | 0.1       |          | 3.364133  |
|      | 0.2       |          | 3.379972  |
|      | 0.5       |          | 3.425116  |
|      | 1         |          | 3.493254  |
|      | 2         |          | 3.612082  |
|      |           | 0.1      | 3.374806  |
|      |           | 0.2      | 3.401936  |
|      |           | 0.5      | 3.481566  |
|      |           | 0.7      | 3.533639  |
|      |           | 1.0      | 3.612082  |

values of suction smooth the fluid flow for both the phases (Fig. 2) because suction rises the skin friction which in turns lowers the velocities of fluid and the dust phases. Influential role of Reynold number is depicted in Fig. 3, as viscous force prevails for the higher values  $Re$ , so fluid motion depreciates. But, on the other hand, high skin friction makes the dust particles to collide more and rises the dust phase velocity. Table 1 shows the effect of flow parameters i.e., particle interaction parameter ( $\beta_v$ ), suction parameter ( $f_w$ ) and the local Reynold number ( $Re$ ) on skin friction coefficient. Enhancement of skin friction is noted for all the parameters, because the involved three parameters generate frictional factor. In Table 2, Nusselt number decreases for larger values of  $Re$ ,  $\gamma$ , while inverse behavior is observed for  $\beta_v$ . Such behavior is justified as Nusselt number goes high with increasing temperature. Ultimately convective heat transfer occurs with rising temperature. The variation of skin friction coefficient  $-g''(1)$  with local Reynold number  $Re$ , particle interaction parameters  $\beta_v$  and the mass concentration parameter  $\gamma$  has been tabulated in Table 3.

#### 4. Conclusions

Numerical study of laminar, steady, viscous and incompressible two dimensional boundary layer flow of dusty fluid along a permeable exponentially stretching cylinder has been carried out in the present draft. Shooting technique by RK-Method of the sixth order is applied on derived equations. Three physical parameters i.e., particle interaction parameter ( $\beta_v$ ), suction parameter ( $f_w$ ) and the local Reynold number ( $Re$ ) are investigated on velocity profile and elaborated through proper graphs and table. Following key points summary the whole findings:

- High particle interaction parameter laminarises the

fluid velocity and raises the dust phase flow.

- Smooth flow attains for both the phases by increasing suction.
- Reynold number lowers the fluid velocity and slightly speed up the dust phase velocity.
- Skin friction elevates for all the involved parameters.

### Declaration of conflicting interests

The author(s) declared no potential conflicts of interest with respect to the research, authorship, and/or publication of this article.

### Acknowledgments

This project was supported by the Deanship of Scientific Research at Prince Sattam Bin Abdulaziz University under research project no. 2019/01/11299.

### References

- Abdulrazzaq, M.A., Fenjan, R.M., Ahmed, R.A. and Faleh, N.M. (2020), "Thermal buckling of nonlocal clamped exponentially graded plate according to a secant function based refined theory", *Steel Compos. Struct., Int. J.*, **35**(1), 147-157. <https://doi.org/10.12989/scs.2020.35.1.147>.
- Agranat, V.M. (1988), "Effect of pressure gradient on friction and heat transfer in a dusty boundary layer", *Fluid Dyn.*, **23**, 729-732. <http://dx.doi.org/10.1007/BF02614150>.
- Akbaş, Ş.D. (2015), "Wave propagation of a functionally graded beam in thermal environments", *Steel Compos. Struct., Int. J.*, **19**(6), 1421-1447. <https://doi.org/10.12989/scs.2015.19.6.1421>.
- Akbaş, Ş.D. (2017a), "Free vibration of edge cracked functionally graded microscale beams based on the modified couple stress theory", *Int. J. Struct. Stab. Dyn.*, **17**(3), 1750033. <https://doi.org/10.1142/S021945541750033X>.
- Akbaş, Ş.D. (2017b), "Nonlinear static analysis of functionally graded porous beams under thermal effect", *Coupled Syst. Mech.*, **6**(4), 399-415. <https://doi.org/10.12989/csm.2017.6.4.399>.
- Akbaş, Ş.D. (2018a), "Large deflection analysis of a fiber reinforced composite beam", *Steel Compos. Struct., Int. J.*, **27**(5), 567-576. <https://doi.org/10.12989/scs.2018.27.5.567>.
- Akbaş, Ş.D. (2018b), "Geometrically nonlinear analysis of a laminated composite beam", *Struct. Eng. Mech., Int. J.*, **66**(1), 27-36. <https://doi.org/10.12989/sem.2018.66.1.027>.
- Akbaş, Ş.D. (2018c), "Post-buckling responses of a laminated composite beam", *Steel Compos. Struct., Int. J.*, **26**(6), 733-743. <https://doi.org/10.12989/scs.2018.26.6.733>.
- Akbaş, Ş.D. (2018c), "Thermal post-buckling analysis of a laminated composite beam", *Struct. Eng. Mech., Int. J.*, **67**(4), 337-346. <https://doi.org/10.12989/sem.2018.67.4.337>.
- Akbaş, Ş.D. (2018d), "Nonlinear thermal displacements of laminated composite beams", *Coupled Syst. Mech.*, **7**(6), 691-705. <https://doi.org/10.12989/csm.2018.7.6.691>.
- Akbaş, Ş.D. (2019a), "Nonlinear static analysis of laminated composite beams under hygro-thermal effect", *Struct. Eng. Mech., Int. J.*, **72**(4), 433-441. <https://doi.org/10.12989/sem.2019.72.4.433>.
- Akbaş, Ş.D. (2019b), "Post-buckling analysis of a fiber reinforced composite beam with crack", *Eng. Fract. Mech.*, **212**, 70-80. <https://doi.org/10.1016/j.engfracmech.2019.03.007>.
- Akbaş, Ş.D. (2019c), "Hygrothermal post-buckling analysis of laminated composite beams", *Int. J. Appl. Mech.*, **11**(1), 1950009. <https://doi.org/10.1142/S1758825119500091>.
- Akbaş, Ş.D. (2019d), "Forced vibration analysis of functionally graded sandwich deep beams", *Coupled Syst. Mech.*, **8**(3), 259-271. <https://doi.org/10.12989/csm.2019.8.3.259>.
- Akbaş, Ş.D. (2020a), "Dynamic responses of laminated beams under a moving load in thermal environment", *Steel Compos. Struct., Int. J.*, **35**(6), 729-737. <https://doi.org/10.12989/scs.2020.35.6.729>.
- Akbaş, Ş.D. (2020b), "Modal analysis of viscoelastic nanorods under an axially harmonic load", *Adv. Nano Res., Int. J.*, **8**(4), 277-282. <http://dx.doi.org/10.12989/anr.2020.8.4.277>.
- Akgoz, B. and Civalek, O. (2011), "Nonlinear vibration analysis of laminated plates resting on nonlinear two-parameters elastic foundations", *Steel Compos. Struct., Int. J.*, **11**(5), 403-421. <https://doi.org/10.12989/scs.2011.11.5.403>.
- Al-Maliki, A.F., Ahmed, R.A., Moustafa, N.M. and Faleh, N.M. (2020), "Finite element based modeling and thermal dynamic analysis of functionally graded graphene reinforced beams", *Adv. Comput. Des., Int. J.*, **5**(2), 177-193. <https://doi.org/10.12989/acd.2020.5.2.177>.
- Avcar, M. (2019), "Free vibration of imperfect sigmoid and power law functionally graded beams", *Steel Compos. Struct., Int. J.*, **30**(6), 603-615. <https://doi.org/10.12989/scs.2019.30.6.603>.
- Baaskaran, N., Ponappa, K. and Shankar, S. (2018), "Assessment of dynamic crushing and energy absorption characteristics of thin-walled cylinders due to axial and oblique impact load", *Steel Compos. Struct., Int. J.*, **28**(2), 179-194. <https://doi.org/10.12989/scs.2018.28.2.179>.
- Batou, B., Nebab, M., Bennai, R., Atmane, H.A., Tounsi, A. and Bouremana, M. (2019), "Wave dispersion properties in imperfect sigmoid plates using various HSDTs", *Steel Compos. Struct., Int. J.*, **33**(5), 699-716. <https://doi.org/10.12989/scs.2019.33.5.699>.
- Benmansour, D.L., Kaci, A., Bousahla, A.A., Heireche, H., Tounsi, A., Alwabli, A.S., Alhebshi, A.M., Al-Ghmady, K. and Mahmoud, S.R. (2019), "The nano scale bending and dynamic properties of isolated protein microtubules based on modified strain gradient theory", *Adv. Nano Res., Int. J.*, **7**(6), 443-457. <https://doi.org/10.12989/anr.2019.7.6.443>.
- Chakrabarti, K.M. (1974), "Note on boundary layer in a dusty gas", *Am. Inst. Aero. Astro. J.*, **12**, 1136-1137. <http://dx.doi.org/10.2514/3.49427>.
- Chen, J., Zhuang, Y., Fang, H., Liu, W., Zhu, L. and Fan, Z. (2019a), "Energy absorption of foam-filled lattice composite cylinders under lateral compressive loading", *Steel Compos. Struct., Int. J.*, **31**(2), 133-148. <https://doi.org/10.12989/scs.2019.31.2.133>.
- Chen, W., Ji, C., Alam, M.M. and Xu, D. (2019b), "Flow-induced vibrations of three circular cylinders in an equilateral triangular arrangement subjected to cross-flow", *Wind Struct., Int. J.*, **29**(1), 43-53. <https://doi.org/10.12989/was.2019.29.1.043>.
- Civalek, Ö. (2017), "Free vibration of carbon nanotubes reinforced (CNTR) and functionally graded shells and plates based on FSDT via discrete singular convolution method", *Compos. Part B Eng.*, **111**, 45-59. <https://doi.org/10.1016/j.compositesb.2016.11.030>.
- Derakhshandeh, J.F. and Alam, M.M. (2020), "Reynolds number effect on the flow past two tandem cylinders", *Wind Struct., Int. J.*, **30**(5), 475-483. <https://doi.org/10.12989/was.2020.30.5.475>.
- Ebrahimi, F., Dabbagh, A., Rabczuk, T. and Tornabene, F. (2019), "Analysis of propagation characteristics of elastic waves in heterogeneous nanobeams employing a new two-step porosity-dependent homogenization scheme", *Adv. Nano Res., Int.*

- J., 7(2), 135-143. <https://doi.org/10.12989/anr.2019.7.2.135>.
- Eltaher, M.A., Almalki, T.A., Ahmed, K.I. and Almitani, K.H. (2019), "Characterization and behaviors of single walled carbon nanotube by equivalent-continuum mechanics approach", *Adv. Nano Res., Int. J.*, 7(1), 39-49. <https://doi.org/10.12989/anr.2019.7.1.039>.
- Imtiaz, M., Hayat, T. and Alsaedi, A. (2016), "MHD convective flow of Jeffrey fluid due to a curved stretching surface with homogeneous-heterogeneous reactions", *PLoS One*, 11(9), e0161641. <https://doi.org/10.1371/journal.pone.0161641>.
- Iqbal, W., Naeem, M.N. and Jalil, M. (2019), "Numerical analysis of Williamson fluid flow along an exponentially stretching cylinder", *AIP Adv.*, 9(5), 055118. <http://dx.doi.org/10.1063/1.5092737>.
- Ishak, A. and Nazar, R. (2009), "Laminar boundary layer flow along a stretching cylinder", *Eur. J. Sci. Res.*, 36(1), 22-29. <https://doi.org/10.5897/IJPS12.093>.
- Ishak, A., Nazar, R. and Pop, I. (2008), "Uniform suction/ blowing effect on flow and heat transfer due to stretching cylinder", *App. Math. Mod.*, 32, 2059-2066. <http://dx.doi.org/10.1016/j.apm.2007.06.036>.
- Karami, B., Janghorban, M. and Tounsi, A. (2017), "Effects of triaxial magnetic field on the anisotropic nanoplates", *Steel Compos. Struct., Int. J.*, 25(3), 361-374. <https://doi.org/10.12989/scs.2017.25.3.361>.
- Karami, B., Janghorban, M. and Tounsi, A. (2018), "Nonlocal strain gradient 3D elasticity theory for anisotropic spherical nanoparticles", *Steel Compos. Struct., Int. J.*, 27(2), 201-216. <https://doi.org/10.12989/scs.2018.27.2.201>.
- Khan, M. and Malik, R. (2015), "Forced convective heat transfer to Sisko fluid flow past a stretching cylinder", *AIP Adv.*, 5(12), 127202. <http://dx.doi.org/10.1063/1.4937346>.
- Konch, J. and Hazarika, G.C. (2017), "Unsteady hydro magnetic flow of dusty fluid over a stretching cylinder with variable viscosity and thermal conductivity", *Int. J. Adv. Sci. Tech.*, 99, 57-70. <http://dx.doi.org/10.14257/ijast.2017.99.05>.
- Imtiaz, M., Hayat, T. and Alsaedi, A. (2016), "Mixed convection flow of Casson nanofluid over a stretching cylinder with convective boundary conditions", *Adv. Power Tech.*, 27(5), 2245-2256. <https://doi.org/10.1016/j.appt.2016.08.011>.
- Loghman, A., Faegh, R.K. and Arefi, M. (2018), "Two-dimensional time-dependent creep analysis of a thick-walled FG cylinder based on first order shear deformation theory", *Steel Compos. Struct., Int. J.*, 26(5), 533-547. <https://doi.org/10.12989/scs.2018.26.5.533>.
- Madani, H., Hosseini, H. and Shokravi, M. (2016), "Differential cubature method for vibration analysis of embedded FG-CNT-reinforced piezoelectric cylindrical shells subjected to uniform and non-uniform temperature distributions", *Steel Compos. Struct., Int. J.*, 22(4), 889-913. <https://doi.org/10.12989/scs.2016.22.4.889>.
- Mahdy, A. (2015), "Heat transfer and flow of a Casson fluid due to a stretching cylinder with the Soret and Dufour effects", *J. Eng. Phys. Therm.*, 88(4), 928-936. <https://doi.org/10.1007/s10891-015-1267-6>.
- Malik, M.Y., Naseer, M., Nadeem, S. and Rehman, A. (2013), "The boundary layer flow of Casson nanofluid over an exponentially stretching cylinder", *Appl. Nanosci.*, 4, 869-873. <https://doi.org/10.1007/s13204-013-0267-0>.
- Malik, M.Y., Hussain, A., Salahuddin, T., Awais, M., Bilal, S. and Khan, F. (2016), "Flow of Sisko fluid over a stretching cylinder and heat transfer with viscous dissipation and variable thermal conductivity: A numerical study", *AIP Adv.*, 6(4), 045118. <https://doi.org/10.1063/1.4948458>.
- Moghaddam, S.H. and Masoodi, A.R. (2019), "Elastoplastic nonlinear behavior of planar steel gabled frame", *Adv. Comput. Des., Int. J.*, 4(4), 397-413. <https://doi.org/10.12989/acd.2019.4.4.397>.
- Naseer, M., Malik, M.Y., Nadeem, S. and Rehman, A. (2014), "The boundary layer flow of hyperbolic tangent fluid over a vertical exponentially stretching cylinder", *Alexandria Eng. J.*, 53, 747-750. <https://doi.org/10.1016/j.aej.2014.05.001>.
- Nath, G. (1970), "Dusty viscous-fluid flow between rotating coaxial cylinders", *Proc. National Ac. Sci. India Sec. A Phys. Sci.*, 40(3), 257.
- Rad, M.H.G., Shahabian, F. and Hosseini, S.M. (2020), "Geometrically nonlinear dynamic analysis of FG graphene platelets-reinforced nanocomposite cylinder: MLPG method based on a modified nonlinear micromechanical model", *Steel Compos. Struct., Int. J.*, 35(1), 77-92. <https://doi.org/10.12989/scs.2020.35.1.077>.
- Rasekh, A., Ganji, D.D., Tavakoli, S., Ehsani, H. and Naeefee, S. (2014), "MHD flow and heat transfer of dusty fluid over a stretching hollow cylinder with a convective boundary conditions", *Heat Trans. Asian Res.*, 43(3), 221-232. <https://doi.org/10.1002/htj.21073>.
- Rebhi, A.D. (2010), "On boundary layer flow of dusty gas from a horizontal circular cylinder", *Braz. J. Chem. Eng.*, 27(4), 653-662. <http://dx.doi.org/10.1590/S0104-66322010000400017>.
- Rehman, A. (2015), "Boundary layer flow and heat transfer of micropolar fluid over a vertical exponentially stretching cylinder", *Appl. Comput. Math.*, 4(6), 424-430. <http://dx.doi.org/10.11648/j.acm.20150406.15>.
- Safaei, B., Khoda, F.H. and Fattahi, A.M. (2019), "Non-classical plate model for single-layered graphene sheet for axial buckling", *Adv. Nano Res., Int. J.*, 7(4), 265-275. <https://doi.org/10.12989/anr.2019.7.4.265>.
- Saffman, P.G. (1962), "On the stability of laminar flow of a dusty gas", *J. Fluid Mech.*, 13, 120-128. <https://doi.org/10.1017/S0022112062000555>.
- Salah, F., Boucham, B., Bourada, F., Benzair, A., Bousahla, A.A. and Tounsi, A. (2019), "Investigation of thermal buckling properties of ceramic-metal FGM sandwich plates using 2D integral plate model", *Steel Compos. Struct., Int. J.*, 33(6), 805-822. <https://doi.org/10.12989/scs.2019.33.6.805>.
- Salahuddin, T., Malik, M.Y., Hussain, A., Awais, M. and Bilal, S. (2017), "Mixed convection boundary layer flow of Williamson fluid with slip conditions over a stretching cylinder by using Keller-box method", *Int. J. Nonlin. Sci. Num. Simul.*, 18(1), 9-17. <https://doi.org/10.1515/ijnsns.2015.0090>.
- Shadravan, S., Ramseyer, C.C. and Floyd, R.W. (2019), "Comparison of structural foam sheathing and oriented strand board panels of shear walls under lateral load", *Adv. Comput. Des., Int. J.*, 4(3), 251-272. <https://doi.org/10.12989/acd.2019.4.3.251>.
- Shahsavari, D., Karami, B. and Janghorban, M. (2019), "Size-dependent vibration analysis of laminated composite plates", *Adv. Nano Res., Int. J.*, 7(5), 337-349. <https://doi.org/10.12989/anr.2019.7.5.337>.
- Sharma, N. and Panda, S.K. (2020), "Multiphysical numerical (FE-BE) solution of sound radiation responses of laminated sandwich shell panel including curvature effect", *Comput. Math. Appl.*, 80(5), 1221-1239. <https://doi.org/10.1016/j.camwa.2020.06.010>.
- Sharma, N., Mahapatra, T.R. and Panda, S.K. (2017a), "Vibro-acoustic behaviour of shear deformable laminated composite flat panel using BEM and the higher order shear deformation theory", *Compos. Struct.*, 180, 116-129. <https://doi.org/10.1016/j.compstruct.2017.08.012>.
- Sharma, N., Mahapatra, T.R. and Panda, S.K. (2017b), "Numerical study of vibro-acoustic responses of un-baffled multi-layered composite structure under various end conditions and experimental validation", *Latin Am. J. Solids Struct.*, 14(8), 1547-1568. <https://doi.org/10.1590/1679-78253830>.

- Sharma, N., Mahapatra, T.R. and Panda, S.K. (2017c), "Vibro-acoustic analysis of un-baffled curved composite panels with experimental validation", *Struct. Eng. Mech., Int. J.*, **64**(1), 93-107. <https://doi.org/10.12989/sem.2017.64.1.093>.
- Sharma, N., Mahapatra, T.R. and Panda, S.K. (2018a), "Numerical analysis of acoustic radiation responses of shear deformable laminated composite shell panel in hygrothermal environment", *J. Sound Vib.*, **431**, 346-366. <https://doi.org/10.1016/j.jsv.2018.06.007>.
- Sharma, N., Mahapatra, T.R. and Panda, S.K. (2018b), "Numerical analysis of acoustic radiation properties of laminated composite flat panel in thermal environment: A higher-order finite-boundary element approach", *Proc. Inst. Mech. Eng. Part C J. Mech. Eng. Sci.*, **232**(18), 3235-3249. <https://doi.org/10.1177/0954406217735866>.
- Sharma, N., Mahapatra, T.R., Panda, S.K. and Hirwani, C.K. (2018c), "Acoustic radiation and frequency response of higher-order shear deformable multilayered composite doubly curved shell panel-an experimental validation", *Appl. Acoust.*, **133**, 38-51. <https://doi.org/10.1016/j.apacoust.2017.12.013>.
- Sharma, N., Mahapatra, T.R., Panda, S.K. and Mehar, K. (2018d), "Evaluation of vibroacoustic responses of laminated composite sandwich structure using higher-order finite-boundary element model", *Steel Compos. Struct., Int. J.*, **28**(5), 629-639. <https://doi.org/10.12989/scs.2018.28.5.629>.
- Sharma, N., Mahapatra, T.R. and Panda, S.K. (2018e), "Thermoacoustic behavior of laminated composite curved panels using higher-order finite-boundary element model", *Int. J. Appl. Mech.*, **10**(2), 1850017. <https://doi.org/10.1142/S1758825118500175>.
- Sharma, N., Mahapatra, T.R. and Panda, S.K. (2019a), "Hygrothermal effect on vibroacoustic behaviour of higher-order sandwich panel structure with laminated composite face sheets", *Eng. Struct.*, **197**, 109355. <https://doi.org/10.1016/j.engstruct.2019.109355>.
- Sharma, N., Mahapatra, T.R. and Panda, S.K. (2019b), "Vibroacoustic analysis of thermo-elastic laminated composite sandwich curved panel: A higher-order FEM-BEM approach", *Int. J. Mech. Mater. Des.*, **15**(2), 271-289. <https://doi.org/10.1007/s10999-018-9426-5>.
- Sharma, N., Mahapatra, T.R., Panda, S.K. and Katariya, P. (2020), "Thermo-acoustic analysis of higher-order shear deformable laminated composite sandwich flat panel", *J. Sandw. Struct. Mater.*, **22**(5), 1357-1385. <https://doi.org/10.1177/1099636218784846>.
- Simsek, M. (2011), "Forced vibration of an embedded single-walled carbon nanotube traversed by a moving load using nonlocal Timoshenko beam theory", *Steel Compos. Struct., Int. J.*, **11**(1), 59-76. <https://doi.org/10.12989/scs.2011.11.1.059>.
- Sofiyev, A.H., Yücel, K., Avcar, M. and Zerín, Z. (2006), "The dynamic stability of orthotropic cylindrical shells with non-homogenous material properties under axial compressive load varying as a parabolic function of time", *J. Reinf. Plast. Compos.*, **25**(18), 1877-1886. <https://doi.org/10.1177/0731684406069914>.
- Wang, C.Y. (1988), "Fluid flow due to a stretching cylinder", *Phys. Fluids*, **31**, 466-468. <https://doi.org/10.1063/1.866827>.
- Wang, C.Y. and Ng, C.O. (2011), "Slip flow due to a stretching cylinder", *Int. J. Nonlin. Mech.*, **46**, 1191-1194. <https://doi.org/10.1016/j.ijnonlinmec.2011.05.04>.
- Yüksel, Y.Z. and Akbaş, Ş.D. (2019), "Buckling analysis of a fiber reinforced laminated composite plate with porosity", *J. Comput. Appl. Mech.*, **50**(2), 375-380. <https://doi.org/10.22059/JCAMECH.2019.291967.448>.